Biochemical Pharmacology 80 (2010) 122–128

Contents lists available at ScienceDirect

Biochemical Pharmacology

journal homepage: www.elsevier.com/locate/biochempharm

Effects of monoamine oxidase inhibitor and cytochrome P450 2D6 status on 5-methoxy-*N*,*N*-dimethyltryptamine metabolism and pharmacokinetics

Hong-Wu Shen, Chao Wu, Xi-Ling Jiang, Ai-Ming Yu *

Department of Pharmaceutical Sciences, School of Pharmacy and Pharmaceutical Sciences, University at Buffalo, The State University of New York, 541 Cooke Hall, Buffalo, NY 14260-1200, USA

ARTICLE INFO

Article history:
Received 26 January 2010
Accepted 24 February 2010

Keywords:
CYP2D6
5-MeO-DMT
MAOI
Pharmacokinetics
Transgenic mouse

ABSTRACT

5-Methoxy-*N*,*N*-dimethyltryptamine (5-MeO-DMT) is a natural psychoactive indolealkylamine drug that has been used for recreational purpose. Our previous study revealed that polymorphic cytochrome P450 2D6 (CYP2D6) catalyzed 5-MeO-DMT *O*-demethylation to produce active metabolite bufotenine, while 5-MeO-DMT is mainly inactivated through deamination pathway mediated by monoamine oxidase (MAO). This study, therefore, aimed to investigate the impact of CYP2D6 genotype/phenotype status and MAO inhibitor (MAOI) on 5-MeO-DMT metabolism and pharmacokinetics. Enzyme kinetic studies using recombinant CYP2D6 allelic isozymes showed that CYP2D6.2 and CYP2D6.10 exhibited 2.6- and 40-fold lower catalytic efficiency (V_{max}/K_m), respectively, in producing bufotenine from 5-MeO-DMT, compared with wild-type CYP2D6.1. When co-incubated with MAOI pargyline, 5-MeO-DMT *O*-demethylation in 10 human liver microsomes showed significantly strong correlation with bufuralol 1′-hydroxylase activities ($R^2 = 0.98$; $P < 0.0001$) and CYP2D6 contents ($R^2 = 0.77$; $P = 0.0007$), whereas no appreciable correlations with enzymatic activities of other P450 enzymes. Furthermore, concurrent MAOI harmaline sharply reduced 5-MeO-DMT depletion and increased bufotenine formation in human CYP2D6 extensive metabolizer hepatocytes. In vivo studies in wild-type and *CYP2D6*-humanized (Tg-*CYP2D6*) mouse models showed that Tg-*CYP2D6* mice receiving the same dose of 5-MeO-DMT (20 mg/kg, i.p.) had 60% higher systemic exposure to metabolite bufotenine. In addition, pretreatment of harmaline (5 mg/kg, i.p.) led to 3.6- and 4.4-fold higher systemic exposure to 5-MeO-DMT (2 mg/kg, i.p.), and 9.9- and 6.1-fold higher systemic exposure to bufotenine in Tg-*CYP2D6* and wild-type mice, respectively. These findings indicate that MAOI largely affects 5-MeO-DMT metabolism and pharmacokinetics, as well as bufotenine formation that is mediated by CYP2D6.

1. Introduction

5-Methoxy-*N*,*N*-dimethyltryptamine (5-MeO-DMT) is a psychoactive indolealkylamine drug found in a variety of plant preparations (e.g., *Virola* snuffs and *Ayahuasca*) and venom of psychoactive toads (e.g., Colorado River *Bufo alvarius*) that have been used for social and religious cultures or recreational purposes [1–3]. 5-MeO-DMT causes physiological, biochemical and behavioral changes and induces visionary and stimulant effects in humans as other hallucinogenic indolealkylamines. Although composite evidences indicate that there is likely a common site of 5-HT_{2A} and other 5-HT_2 receptors in the central nervous system responsible for the actions of indolealkylamine hallucinogens [4], 5-MeO-DMT has been shown to act mainly through the 5-HT_{1A} receptor [5–7]. Rather, 5-MeO-DMT is known as a nonselective 5-HT receptor agonist, and both 5-HT_{1A} and 5-HT_2 receptors seem to be involved in its complex pharmacological and toxicological effects [8].

5-MeO-DMT had been an uncontrolled substance in the United States of America (USA), in contrast to its chemically and pharmacologically related drugs, 5-hydroxy-*N*,*N*-dimethyltryptamine (bufotenine), *N*,*N*-dimethyltryptamine (DMT), 5-methoxy-*N*,*N*-diisopropyltryptamine (5-MeO-DiPT) and α-methyltryptamine (AMT) that all have been Schedule I controlled drugs for years. 5-MeO-DMT was available on the Internet both as a natural product in plant or animal preparations, as well as a synthetic compound. The abuse of 5-MeO-DMT is evident from intoxications reported in hospitals in recent years, which include the co-abuse with

Abbreviations: CYP2D6, cytochrome P450 2D6; 5-MeO-DMT, 5-methoxy-*N*,*N*-dimethyltryptamine; MAOI, monoamine oxidase inhibitor; DDI, drug–drug interactions; EM, extensive metabolizer; PM, poor metabolizer; HLM, human liver microsomes; HPLC, high performance liquid chromatography; LC–MS/MS, liquid chromatography tandem mass spectrometry.

* Corresponding author. Tel.: +1 716 645 4817; fax: +1 716 645 3693.
E-mail address: aimingyu@buffalo.edu (A.-M. Yu).

0006-2952/$ – see front matter © 2010 Elsevier Inc. All rights reserved.
doi:10.1016/j.bcp.2010.02.020

monoamine oxidase (MAO) inhibitor such as harmaline [9] and a fatal case of intoxication [10]. On August 21, 2009, the Drug Enforcement Administration issued a notice of intention to place 5-MeO-DMT into Schedule I of the Controlled Substances Act in the USA [11].

As a tryptamine derivative, 5-MeO-DMT is primarily eliminated through oxidative deamination initiated by monoamine oxidase-A (MAO-A). Therefore, co-administration of a MAO-A inhibitor (MAOI) such as harmaline likely alters the metabolic elimination and pharmacokinetic profile of 5-MeO-DMT [3]. In addition, animal studies have shown that *O*-demethylation is another major metabolic pathway for ^{14}C-labeled 5-MeO-DMT [12]. Of particular note, the *O*-demethylated metabolite, bufotenine, has been shown as a potent ligand for 5-HT_{2A} receptor with an affinity up to 10-fold higher than 5-MeO-DMT itself [13]. Bufotenine is at least equally active as 5-MeO-DMT when directly injected into animal cerebral ventricle [14]. Our previous studies using recombinant human cytochrome P450 (CYP or P450) isozymes have revealed that formation of bufotenine from 5-MeO-DMT is primarily catalyzed by CYP2D6 drug-metabolizing enzyme [15]. Since CYP2D6 is well recognized for its genetic polymorphism and clinical importance [16,17], delineation of the impact of CYP2D6 genotype/phenotype on bufotenine production from 5-MeO-DMT would advance our understanding of 5-MeO-DMT pharmacology, as well as risk factors in 5-MeO-DMT intoxication. Therefore, present study aimed to employ both in vitro and in vivo models to define the effects of CYP2D6 status and MAOI on 5-MeO-DMT metabolism and pharmacokinetics.

2. Materials and methods

2.1. Chemicals and materials

5-MeO-DMT oxalate, harmaline hydrochloride dihydrate, pargyline, 5-methyl-*N*,*N*-dimethyltryptamine (5-Me-DMT), reduced nicotinamide adenine dinucleotide phosphate (NADPH) and β-glucuronidase were purchased from Sigma–Aldrich (St. Louis, MO). Bufotenine standard was bought from Cambridge Isotope Laboratories (Andover, MA). Cryopreserved human hepatocytes (coded PFM, ETR, VTA, GNG, KRM, VEN, KRJ, HH183 and HH169), human liver microsomes (HLM; coded H030, H006, H112, H066, H089, H056, H003, H088, H043, and H093), InVitroGRO HT Medium, KHB buffer and Torpedo Antibiotic Mix were purchased from Celsis (Chicago, IL) or BD Biosciences Discovery Labware (Woburn, MA). CYP2D6 phenotype or genotype of each hepatocyte sample was provided by the manufacturers, which was then classified as CYP2D6 extensive metabolizer (EM) or poor metabolizer (PM) hepatocytes as described [18]. CYP2D6 allelic isoforms were expressed using baculovirus-mediated system and purified as reported [19–21]. All other reagents or organic solvents used were either analytical or high performance liquid chromatography (HPLC) grade.

2.2. Drug metabolism by recombinant CYP2D6 allelic isozymes

Incubation reactions with CYP2D6 allelic isoforms were conducted in 100 mM potassium phosphate buffer (pH 7.4) in a final volume of 200 μL at 37 °C, as described [19–21]. Particularly, each reaction consisted of 0.2 μM of CYP2D6, 0.4 μM of P450 reductase, 10 μg of L-α-dilaurylphosphatidylcholine and 10–1000 μM of 5-MeO-DMT. Incubations were carried out for 5 min for CYP2D6.1 and CYP2D6.2, and 20 min for CYP2D6.10, respectively. All reactions were initiated by the addition of NADPH (1 mM final concentration) and terminated by 10 μL of 70% perchloric acid. All reactions were conducted in triplicate. The mixture was centrifuged at 14,000 × *g* for 5 min, and the supernatant was injected for HPLC analysis.

2.3. Drug metabolism in human liver microsomes

Each incubation reaction was carried out in 100 mM potassium phosphate buffer (pH 7.4), in a final volume of 200 μL, consisting of liver microsomes (0.5–1.0 mg microsomal protein/mL) from individual donors ($N = 10$), 5-MeO-DMT (10 μM) and pargyline (20 μM). Reactions were initiated by the addition of 20 μL of 10 mM NADPH after a 5-min pre-incubation at 37 °C. After incubated for 10 min, the reaction was terminated by 10 μL of 70% perchloric acid. All reactions were performed in duplicate. The mixture was cooled on ice for 10 min, and centrifuged at 14,000 × *g* for 10 min. The supernatant was transferred to a new vial, and injected for HPLC analysis.

2.4. Drug metabolism in human hepatocytes

Metabolic reactions were conducted as described [18]. Briefly, reaction was initiated by mixing the same volume of drug solution (5-MeO-DMT alone or 5-MeO-DMT plus harmaline in KHB buffer) and resuspended hepatocytes. Cells were incubated at 37 °C, 5% carbon dioxide and saturating humidity. All incubations were performed in duplicate for each hepatocyte sample. Each well consisted of 2 μM of individual drugs and 0.5×10^6 cells/mL of hepatocytes in a total volume of 1.6 mL. Forty microliters of media were aliquoted at different time points (0–90 min) and snap-frozen in liquid nitrogen. Upon analyses, samples were thawed on ice and 40 μL were digested with β-glucuronidase at 37 °C for 3 h. The mixtures were then deproteinized with 5 μL of ice-cold perchloric acid (70%) and centrifuged at 14,000 × *g* for 10 min. The supernatant was transferred to a new vial and injected for HPLC quantification of drugs and metabolites.

2.5. Animals and pharmacokinetic studies

All mice were housed under the controlled temperature (20 ± 2 °C), relative humidity (50–60%) and lighting (lights on 6:00 a.m.–6:00 p.m.), with food and water provided *ad libitum*. All animal procedures were approved by the Institutional Animal Care and Use Committee (IACUC) at University at Buffalo. To examine the effect of CYP2D6 status on bufotenine formation, age-matched adult (8 weeks old) wild-type FVB/N and Tg-*CYP2D6* mice [22] weighting 25–30 g were treated intraperitoneally (i.p.) with 20 mg/kg of 5-MeO-DMT. To investigate the impact of MAOI on 5-MeO-DMT pharmacokinetics, wild-type and Tg-*CYP2D6* mice (8 weeks old, 25–30 g) were administered i.p. with 2 mg/kg of 5-MeO-DMT, with or without pretreatment with 5 mg/kg of harmaline (i.p., 15 min before). Blood samples were collected from individual mice at different time points (0–240 min, $N = 4$ per time point) after 5-MeO-DMT administration. Serum was isolated with a serum separator (Becton Dickinson, Franklin Lakes, NJ) and stored at −80 °C before analysis. Sixty microliters of ice-cold acetonitrile containing 50 nmol/L of 5-Me-DMT (internal standard) were added into 20 μL of serum sample to precipitate protein. After centrifuged at 14,000 × *g* for 10 min, the supernatant was injected for liquid chromatography tandem mass spectrometry (LC–MS/MS) analysis.

2.6. HPLC and LC–MS/MS quantification

All in vitro incubations were subjected to HPLC quantification of bufotenine and 5-MeO-DMT. The Agilent 1100 series HPLC system (Palo Alto, CA) consisting of an online vacuum degasser, quaternary pump, autosampler, thermostat controlled column compartment, fluorescence detector and diode-array detector was controlled by Agilent ChemStation software. A Regis REXCHROM phenyl column (250 mm × 4.6 mm, 5 μm; Morton Grove, IL) was used for the separation of 5-MeO-DMT and

bufotenine under the conditions described previously [15]. The calibration linear range for 5-MeO-DMT and bufotenine was 2–100 pmol on-column. Intra-day and inter-day coefficients of variation were less than 10% for each analyte.

LC–MS/MS quantification of 5-MeO-DMT and bufotenine in mouse serum samples was performed with a Shimadzu prominence HPLC (Kyoto, Japan) coupled to an API 3000 turbo ionspray ionization triple–quadrupole mass spectrometer (Applied Biosystems, Foster City, CA). Separation of analytes was achieved using a 3 μm Phenomenex phenyl-hexyl column (50 mm × 4.6 mm, Torrance, CA). Validated LC–MS/MS method was reported elsewhere [23].

2.7. Data analysis

All values were expressed as mean ± SD when experiments were carried out using different samples, or mean ± SEM when experiments conducted multiple times using the same sample. Michaelis–Menten kinetic parameters, K_m and V_{max}, were estimated by nonlinear regression (GraphPad Prism 5, San Diego, CA). Intrinsic clearance (CL_{int}) was calculated by dividing V_{max} by K_m. Linear regression (Prism 5) was carried out to investigate correlation of 5-MeO-DMT *O*-demethylase with P450 isoform-selective reactions. Squared correlation coefficient (R^2) was used to define the strength of a relationship, and statistical significance was noted when the probability (*P*-value) was less than 0.05 ($P < 0.05$). 5-MeO-DMT depletion data from hepatocyte studies were fit to a mono-exponential decay kinetic model [$C_{(t)} = C_0 e^{-kt}$] (Prism 5) where C_0 is the initial drug concentration in incubation, and k is the terminal depletion rate constant. In vitro clearance (CL_{int}) was calculated by dividing the dose (D_0) by the area under the concentration–time curve (AUC), and normalized with cell variability, as described [18].

Pharmacokinetic parameters were estimated by noncompartmental analyses (WinNonLin v5.0, Pharsight, Mountain View, CA). The maximum serum concentrations (C_{max}) and the time to reach peak serum concentration (T_{max}) were observed values with no interpolation. The area under serum concentration–time curve up to the last measured time point ($AUC_{0\to t}$) was calculated by the trapezoidal rule. The $AUC_{0\to\infty}$ was generated by extrapolating the $AUC_{0\to t}$ to infinity using the last measured concentration and the terminal slope (λ) of linear regression from log concentration versus time relationship. The elimination half-life ($T_{1/2}$) was calculated using the relationship of 0.693/λ. The mean residence time (MRT) was calculated by dividing the total area under the first moment of the drug concentration curve ($AUMC_{0\to\infty}$) by $AUC_{0\to\infty}$. Depending on the number of groups and variances, values were compared with unpaired Student's *t*-test, one-way ANOVA analysis followed by Dunnett's test, or two-way ANOVA (Prism 5). Difference was considered statistically significant if $P < 0.05$.

3. Results

3.1. CYP2D6 allelic isoforms had distinct enzymatic capacities in producing bufotenine from 5-MeO-DMT

To assess the effect of CYP2D6 status on 5-MeO-DMT *O*-demethylation, we first compared enzymatic activities of recombinant CYP2D6.1, CYP2D6.2, and CYP2D6.10 allelic isoforms in producing the active metabolite bufotenine. All isoforms produced bufotenine from 5-MeO-DMT, exhibiting one-enzyme Michaelis–Menten kinetics (Fig. 1). The wild-type CYP2D6.1 showed the lowest K_m value (29.3 ± 4.2 μM), followed by CYP2D6.2 (85.0 ± 19.4 μM) and CYP2D6.10 (947 ± 355 μM). With a similar V_{max} value as that for CYP2D6.2 (Table 1), CYP2D6.1 exhibited the highest catalytic activity (CL_{int}, 0.44 μL/pmol P450/min) and CYP2D6.10 had the lowest enzymatic activity (0.011 μL/pmol P450/min) (Table 1). Overall,

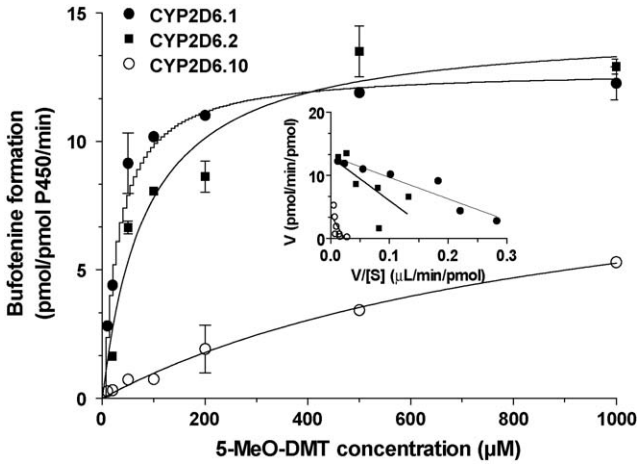

Fig. 1. Michaelis–Menten plots of bufotenine production from 5-MeO-DMT catalyzed by recombinant CYP2D6.1, CYP2D6.2 and CYP2D6.10 allelic isoforms. Metabolite was quantified by HPLC assay. Values represent mean ± SEM. Inserted are the transformed Eadie–Hofstee plots.

Table 1
Enzyme kinetic parameters estimated for bufotenine production from 5-MeO-DMT catalyzed by CYP2D6 allelic isoforms. Data were fit to one-enzyme Michaelis–Menten equation (GraphPad Prism 5). Values represent mean ± SEM.

Allelic isoform	K_m (μM)	V_{max} (pmol/pmol P450/min)	CL_{int} (μL/pmol P450/min)
CYP2D6.1	29.3 ± 4.2	12.8 ± 0.4	0.44
CYP2D6.2	85.0 ± 19.4	14.4 ± 0.9	0.17
CYP2D6.10	947 ± 355	10.3 ± 2.2	0.011

CYP2D6.2 showed 2.6-fold lower 5-MeO-DMT *O*-demethylase activity and CYP2D6.10 showed 40-fold lower activity, when compared with wild-type CYP2D6.1 enzyme. The results indicate that different CYP2D6 allelic isoforms have distinct catalytic efficiencies in producing bufotenine from 5-MeO-DMT.

3.2. Blockage of MAO activity led to a strong correlation between 5-MeO-DMT O-demethylation and CYP2D6 activity in human liver microsomes

To evaluate the role of CYP2D6 in 5-MeO-DMT *O*-demethylation pathway in HLM, we conducted a correlation study (Table 2). As a tryptamine derivative, 5-MeO-DMT was mainly deaminated by MAO-A that was present in the HLM [24]. As a result, no significant correlation was observed between 5-MeO-DMT *O*-demethylase and CYP2D6 activities in HLMs (data not shown). When deamination metabolism was blocked by MAOI pargyline,

Table 2
Correlation between 5-MeO-DMT *O*-demethylase activity and individual P450 form-selective enzyme activities in HLM samples ($N = 10$). Pargyline was co-incubated with 5-MeO-DMT to block the deamination oxidation of 5-MeO-DMT.

Enzyme activity	P450	R^2	*P*
Phenacetin *O*-deethylase	CYP1A2	0.01	0.81
Coumarin 7-hydroxylase	CYP2A6	0.48	0.03
(S)-mephenytoin *N*-demethylase	CYP2B6	<0.01	0.95
Paclitaxel 6α-hydroxylase	CYP2C8	0.10	0.39
Diclofenac 4′-hydroxylase	CYP2C9	0.09	0.41
(S)-mephenytoin 4′-hydroxylase	CYP2C19	0.09	0.41
Bufuralol 1′-hydroxylase	CYP2D6	0.98	<0.0001
Chlorzoxazone 6-hydroxylase	CYP2E1	0.18	0.21
Testosterone 6β-hydroxylase	CYP3A4/5	0.07	0.48
Lauric acid 12-hydroxylase	CYP4A	<0.01	0.90
CYP2D6 content		0.77	0.0007

5-MeO-DMT *O*-demethylase activities in 10 HLM samples showed a strong and significant correlation with CYP2D6-catalyzed bufuralol 1′-hydroxylase activities (R^2 = 0.98; $P < 0.0001$), as well as immunoblot-estimated CYP2D6 contents (R^2 = 0.77; P = 0.0007) (Table 2) In contrast, 5-MeO-DMT *O*-demethylase activity exhibited no or minimal correlation ($R^2 < 0.50$) with other P450 isoform-selective activity. The results suggest that CYP2D6 is the major enzyme contributing to 5-MeO-DMT *O*-demethylation, and CYP2D6 status could influence the level of bufotenine formation.

3.3. MAOI harmaline significantly reduced 5-MeO-DMT depletion and increased bufotenine formation in human hepatocytes

We then employed phenotyped/genotyped human hepatocytes to delineate the effects of MAOI and CYP2D6 status on 5-MeO-DMT metabolism and bufotenine formation. As expected, 5-MeO-DMT depletion was not different between CYP2D6 EM and PM hepatocytes (Fig. 2 and Table 3) since MAO-A-mediated deamination is the major metabolic pathway for 5-MeO-DMT. In contrast, concurrent MAOI harmaline markedly reduced 5-MeO-DMT depletion in both CYP2D6 EM and PM hepatocytes (Fig. 2), which was also manifested by the estimated kinetic parameters (Table 3). For instance, in vitro CL_{int} values of 5-MeO-DMT in CYP2D6 EM hepatocytes were reduced over 24-fold by co-administered harmaline (92.1 ± 32.1 μL/min/10^6 cells for 5-MeO-DMT alone vs. 3.72 ± 0.68 μL/min/10^6 cells for 5-MeODMT with harmaline). Due to the absence of CYP2D6 activity, CYP2D6 PM hepatocytes could not produce detectable bufotenine, even co-incubated with harmaline. The active metabolite bufotenine was only detected in incubations with CYP2D6 EM hepatocytes, whose levels were also elevated by concurrent harmaline (Fig. 2). It was also noted that harmaline metabolism was significantly slower in CYP2D6 PM hepatocytes (data not shown), consistent with our previous findings [18]. The results not only support that bufotenine formation is dependent on CYP2D6 status but also indicate that significant metabolic drug–drug interactions (DDI) may occur between MAOI and 5-MeO-DMT.

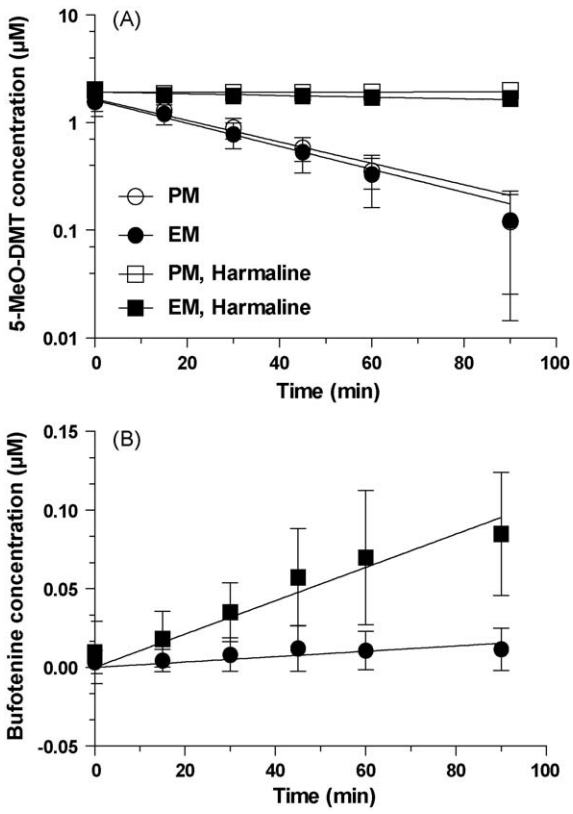

Fig. 2. Effects of harmaline and CYP2D6 status on the depletion of 5-MeO-DMT (A) and formation of bufotenine (B) in human hepatocytes. Samples were collected at different time points, and substrate and metabolite concentrations were quantified by HPLC analyses. Values represent mean ± SD (CYP2D6 EM, N = 5; PM, N = 4). 5-MeO-DMT depletion was not different between CYP2D6 EM and PM hepatocytes. In contrast, significant difference ($P < 0.0001$) was noted for the impact of harmaline on 5-MeO-DMT depletion in both CYP2D6 EM and PM hepatocytes, as well as the effect of CYP2D6 status on bufotenine production in CYP2D6 EM hepatocytes.

3.4. Systemic exposure to bufotenine metabolite was higher in Tg-CYP2D6 mice than wild-type mice treated with a high dose of 5-MeO-DMT

The Tg-*CYP2D6* and wild-type control mouse models [22] were used to investigate the effect of CYP2D6 status on bufotenine production in a whole body system. After i.p. administration of 20 mg/kg 5-MeO-DMT, serum 5-MeO-DMT and bufotenine concentrations were monitored in the two genotyped mice (Fig. 3). The data showed that 5-MeO-DMT pharmacokinetic parameters (C_{max}, T_{max}, AUC, $T_{1/2}$, and MRT) were similar in Tg-*CYP2D6* and wild-type mice (Table 4). In contrast, Tg-*CYP2D6* mice had higher systemic exposure ($AUC_{0-\infty}$, 23.4 ± 1.0 μmol min/L) to bufotenine than wild-type mice (14.4 ± 0.8 μmol min/L). These results indicate that

Table 3
Kinetic parameters of 5-MeO-DMT depletion in human hepatocytes in the presence and absence of harmaline. Mean values from duplicated experiments were fit to the mono-exponential decay model. Intrinsic clearance (CL_{int}) value was corrected with cell variability for each hepatocyte sample. CL_{int} values (mean ± SD) of 5-MeO-DMT depletion are comparable between CYP2D6 EM and PM hepatocytes, whereas the values are significantly reduced when 5-MeO-DMT was co-incubated with harmaline, as compared with 5-MeO-DMT only ($P < 0.001$, Student's t-test).

CYP2D6 status	Hepatocytes	5-MeODMT alone			5-MeODMT with harmaline		
		K_e ($\times 10^{-3}$ min^{-1})	In vitro $T_{1/2}$ (min)	In vitro CL_{int} (μL/min/10^6 cells)	K_e ($\times 10^{-3}$ min^{-1})	In vitro $T_{1/2}$ (min)	In vitro CL_{int} (μL/min/10^6 cells)
PM	1	18.6	37.2	66.5	0.86	803	2.22
	2	25.1	27.6	95.8	Cannot be estimated		
	3	21.5	32.2	88.0	Cannot be estimated		
	4	26.5	26.1	77.4	Cannot be estimated		
	Mean	22.9	30.8	81.9	0.86	803	2.22
	SD	3.6	5.0	12.8			
EM	1	21.4	32.4	92.3	2.59	268	2.76
	2	23.2	29.9	88.7	1.41	493	3.73
	3	27.3	25.4	141	2.63	264	3.79
	4	20.0	34.7	51.0	1.95	256	4.68
	5	33.3	20.8	87.4	0.61	1150	3.64
	Mean	25.0	28.6	92.1	1.84	486	3.72
	SD	5.4	5.6	32.1	0.85	384	0.68

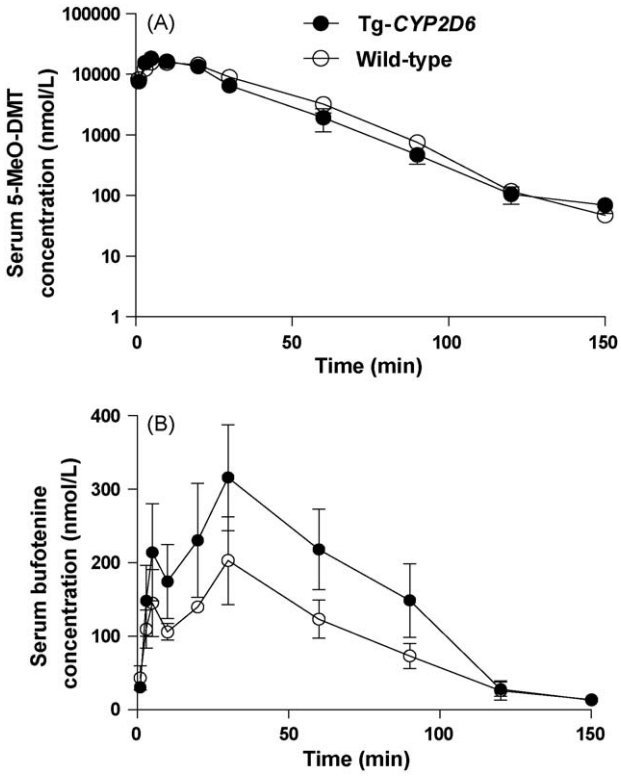

Fig. 3. Serum 5-MeO-DMT (A) and bufotenine (B) concentration versus time profiles in wild-type and Tg-*CYP2D6* mice dosed i.p. with 20 mg/kg of 5-MeO-DMT. Drug and metabolite concentrations were determined by LC–MS/MS method. Values represent mean ± SD (N = 4 at each time point).

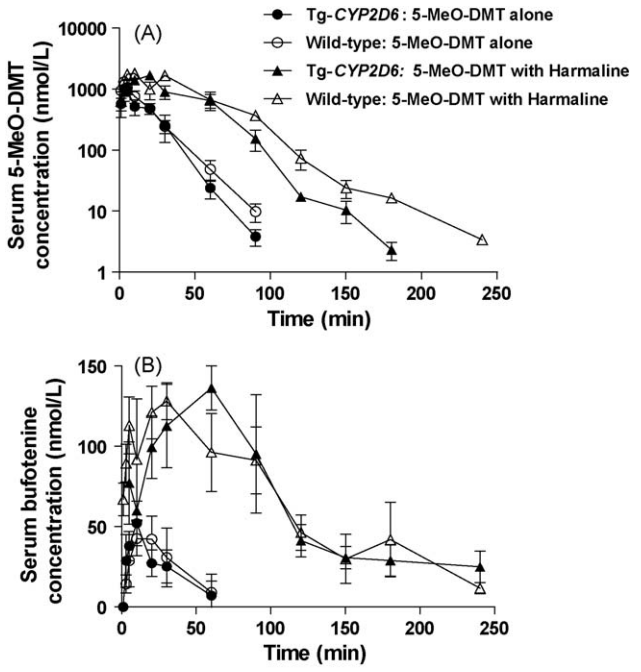

Fig. 4. Serum 5-MeO-DMT (A) and bufotenine (B) concentration versus time profiles in wild-type and Tg-*CYP2D6* mice dosed i.p. with 2 mg/kg of 5-MeO-DMT alone or with 5 mg/kg of harmaline. 5-MeO-DMT and bufotenine levels were determined by LC–MS/MS method. Values represent mean ± SD (N = 4 at each time point).

subjects expressing functional CYP2D6 enzyme have an enhanced capacity in 5-MeO-DMT *O*-demethylation, leading to higher exposure to the active metabolite bufotenine.

3.5. Co-administration of MAOI harmaline resulted in an increased and prolonged systemic exposure to 5-MeO-DMT and bufotenine in mice

To further assess the effects of MAOI and CYP2D6 status on 5-MeO-DMT pharmacokinetics and bufotenine formation, Tg-*CYP2D6* and wild-type mice were administered with a low dose of 5-MeO-DMT (2 mg/kg, i.p.) with and without pretreatment of harmaline (5 mg/kg, i.p.). As expected, both wild-type and Tg-*CYP2D6* mice pretreated with MAOI harmaline were subjected to a sharply increased and prolonged systemic exposure to 5-MeO-DMT and bufotenine (Fig. 4), as manifested by the change of $AUC_{0\rightarrow\infty}$, C_{max}, $T_{1/2}$, and/or MRT values (Table 5). For example, the C_{max}, $AUC_{0\rightarrow\infty}$ and MRT of 5-MeO-DMT were increased significantly about 1.4-, 4.4-, and 2.1-fold, respectively, in wild-type mice co-administered with harmaline. Meanwhile, the C_{max}, $AUC_{0\rightarrow\infty}$ and MRT of bufotenine were increased about 2.6-, 6.1-, and 1.8-fold, respectively, in wild-type mice after co-administration of 5-MeO-DMT with harmaline. Interestingly, Tg-*CYP2D6* mice co-administered with 2 mg/kg 5-MeO-DMT and 5 mg/kg harmaline showed lower systemic exposure ($AUC_{0\rightarrow\infty}$) to 5-MeO-DMT than wild-type mice with the same treatment (Fig. 4 and Table 5). As a result, overall exposure ($AUC_{0\rightarrow\infty}$) to bufotenine metabolite was only 15.1 ± 2.9% of the exposure to 5-MeO-DMT in wild-type mice, whereas it was 24.0 ± 3.3% in Tg-*CYPD6* mice. The results

Table 4
Pharmacokinetic parameters estimated for 5-MeO-DMT and its active metabolite, bufotenine, in wild-type and Tg-*CYP2D6* mice, after i.p. administration of 20 mg/kg 5-MeO-DMT.

	5-MeO-DMT		Bufotenine	
	Wild-type	Tg-*CYP2D6*	Wild-type	Tg-*CYP2D6*
C_{max} (μmol/L)	18.3 ± 2.8	18.7 ± 0.9	0.210 ± 0.054	0.331 ± 0.064*
T_{max} (min)	7.5 ± 2.9	6.3 ± 2.5	21.3 ± 11.8	27.5 ± 5.0
$AUC_{0\rightarrow\infty}$ (μmol min/L)	650 ± 78	568 ± 72	14.4 ± 0.8	23.4 ± 1.0*
$T_{1/2}$ (min)	13.4 ± 1.0	13.4 ± 1.4	25.4 ± 5.3	18.5 ± 1.5
MRT (min)	27.2 ± 3.2	23.1 ± 3.6	55.8 ± 6.7	52.8 ± 3.4

* $P < 0.05$, compared with the corresponding values in wild-type mice.

Table 5
Pharmacokinetic parameters estimated for 5-MeO-DMT in wild-type and Tg-*CYP2D6* mice, after administration of 2 mg/kg 5-MeO-DMT alone or in combination with 5 mg/kg harmaline.

	5-MeO-DMT alone		5-MeO-DMT with harmaline	
	Wild-type	Tg-*CYP2D6*	Wild-type	Tg-*CYP2D6*
5-MeO-DMT				
C_{max} (μmol/L)	1.36 ± 0.16	1.19 ± 0.33	1.97 ± 0.15[a]	1.68 ± 0.39
T_{max} (min)	5.3 ± 3.3	5.8 ± 3.0	7.5 ± 2.9	17.5 ± 5.0[a,b]
$AUC_{0\rightarrow\infty}$ (μmol min/L)	25.1 ± 1.3	21.1 ± 2.3[b]	110 ± 15[a]	76.2 ± 12.5[a,b]
$T_{1/2}$ (min)	19.5 ± 12.2	14.7 ± 9.0	17.5 ± 4.5	24.6 ± 5.0
CL (L/min)	0.37 ± 0.02	0.44 ± 0.05[b]	0.085 ± 0.010[a]	0.12 ± 0.02[a,b]
MRT (min)	19.1 ± 3.5	17.4 ± 3.2	40.2 ± 2.5[a]	35.4 ± 2.4[a,b]
Bufotenine				
C_{max} (nmol/L)	51.4 ± 9.1	53.0 ± 13.0	132 ± 9[a]	138 ± 14[a]
T_{max} (min)	11.3 ± 6.3	8.8 ± 2.5	18.8 ± 10.3	60.0 ± 24.0[a,b]
$AUC_{0\rightarrow\infty}$ (μmol min/L)	2.69 ± 1.21	1.82 ± 0.74	16.3 ± 1.4[a]	18.0 ± 1.5[a]
$T_{1/2}$ (min)	33.0 ± 26.0	20.7 ± 9.8	66.2 ± 10.8	73.8 ± 15.2[a]
MRT (min)	54.9 ± 37.2	33.7 ± 14.8	100 ± 6	126 ± 26[a]
$\frac{AUC(bufotenine)}{AUC(5-MeO-DMT)}$	10.5 ± 4.4%	8.5 ± 2.8%	15.1 ± 2.9%	24.0 ± 3.3%[a,b]

[a] $P < 0.05$, compared with the corresponding values for the same genotype mice treated with 5-MeO-DMT alone.

[b] $P < 0.05$, compared with the corresponding values for wild-type mice received the same treatment.

suggest that concurrent MAOI largely affects 5-MeO-DMT pharmacokinetics and its active metabolite bufotenine, and the latter could be altered by CYP2D6 status.

4. Discussion

5-MeO-DMT belongs to a group of abused tryptamine derivatives that include several Schedule I controlled drugs, bufotenine, DMT, 5-MeO-DiPT and AMT [3]. In vitro binding studies have shown that 5-MeO-DMT binds to 5-HT_{2A} receptor [6] and 5-HT_{1A} receptor with high affinity [13], supporting the importance for both 5-HT_{1A} and 5-HT_{2A} in overall pharmacological effects of 5-MeO-DMT [7,8]. Our previous in vitro studies suggest that 5-MeO-DMT may be *O*-demethylated by polymorphic CYP2D6 to produce bufotenine [15,17], besides the major deamination pathway. Since bufotenine shows about 10-fold higher affinity to 5-HT_{2A} receptor than 5-MeO-DMT itself [13], bufotenine formed from 5-MeO-DMT may contribute at least partly to the apparent non-selectivity of 5-MeO-DMT [23]. The present in vivo studies showed that wild-type and Tg-*CYP2D6* mice treated with 5-MeO-DMT were inevitably exposed to bufotenine. Depending on CYP2D6 status, MAOI co-administration and 5-MeO-DMT dosage, systemic exposure (AUC) to bufotenine was 2–24% of the systemic exposure to 5-MeO-DMT (Tables 4 and 5), indicating potential involvement of bufotenine metabolite in complex pharmacological effects of 5-MeO-DMT.

The clinical significance of CYP2D6 polymorphism is well recognized since CYP2D6 is involved in the metabolism of many therapeutic drugs and substances of abuse [3,16,17]. Individuals with different CYP2D6 allelic variations could have diverse metabolic capacities and show distinct responses to the same xenobiotic drug. As an example, the CYP2D6 PMs were found to have significantly higher and longer exposure to 3,4-methylenedioxymethamphetamine (MDMA, "ecstasy"), an amphetamine drug of abuse, than CYP2D6 EMs [25]. Current study showed that, compared to wild-type CYP2D6.1, CYP2D6.2 and CYP2D6.10 allelic isoforms had much lower catalytic activities in producing bufotenine from 5-MeO-DMT (Table 1), consistent with our previous findings [19,21]. Our data also indicated that human CYP2D6 PM hepatocytes lacking functional CYP2D6 activity could not produce detectable bufotenine, whereas CYP2D6 EM hepatocytes could (Fig. 2). Following the administration of a high dose of 5-MeO-DMT (20 mg/kg, i.p.), Tg-*CYP2D6* mice showed significantly higher systemic exposure (AUC) to the active metabolite bufotenine than wild-type mice (Table 4). As Tg-*CYP2D6* mice differ from wild-type mice in the expression of functional CYP2D6 enzyme [22], these findings have prompted the expectation that subjects with regular or increased CYP2D6 activity would have more complex drug effects induced by bufotenine metabolite.

Since 5-MeO-DMT is primarily inactivated through MAO-A-mediated deamination pathway, co-abuse of 5-MeO-DMT with MAOI harmaline [9] is anticipated to induce metabolic DDI and increase the risk of 5-MeO-DMT intoxication. Harmaline is found in the seeds of *Peganum harmala* (Syrian rue) and is one of the major psychotropic ingredients in recreational beverage *Ayahuasca*. Harmaline is a reversible competitive inhibitor for MAO-A, and shows a very low K_i value of 48 nM to purified human MAO-A [26]. Our data indicated that concurrent harmaline significantly decreased 5-MeO-DMT depletion in both human CYP2D6 EM and PM hepatocytes (Fig. 2 and Table 3). Furthermore, pretreatment of harmaline led to a prolonged (MRT) and increased systemic exposure (AUC) to 5-MeO-DMT in Tg-*CYP2D6* and wild-type mice (Table 5). Indeed, human self-experiments of 5-MeO-DMT suggest that psychedelic effects of 5-MeO-DMT are roughly doubled when concomitantly used (intranasally or sublingually) with nonfunctional dose of harmaline or another β-carboline alkaloid harmine [27]. When used with 40 mg of harmaline in *pharmahuasca*, orally inactive dose of 10 mg 5-MeO-DMT shows nearly equal intensity of psychonautic effects as intranasally or sublingually dosed 10 mg 5-MeO-DMT. Furthermore, recent animal studies have demonstrated that pretreatment of behaviorally inactive dose of harmaline shifts the function of 5-MeO-DMT on locomotor activity to a biphasic pattern (initially reduced and then increased as time progresses) [28]. Together, combined use of harmaline alters the pharmacological outcome of 5-MeO-DMT that may be due to the change of 5-MeO-DMT pharmacokinetics, which could be true to other tryptamine derivatives including 5-MeO-DiPT (Foxy) [29–31].

In addition, blockage of MAO-mediated deamination metabolism of 5-MeO-DMT may cause variation in other metabolic pathways. The prior treatment of MAOI iproniazid or pargyline has been shown to redirect the metabolism of 5-MeO-DMT, resulting in higher levels of other metabolites in rat urine [32,33]. Compared with 5-MeO-DMT alone, co-incubation of 5-MeO-DMT with harmaline sharply increased the production of active metabolite bufotenine in human CYP2D6 EM hepatocytes (Fig. 2). It is noteworthy that bufotenine is also subjected to MAO-A-mediated metabolism [34]. The increase of bufotenine metabolite may be attributed not only to the change of 5-MeO-DMT metabolism but also to the inhibition of bufotenine deamination. In addition, bufotenine formation (C_{max} and AUC) was markedly increased in Tg-*CYP2D6* and wild-type mice in vivo when pretreated with harmaline (Table 5). Because bufotenine has been proved to be psychoactive in animal studies and human self-experiments [1,14] and even more potent in binding to 5-HT_{2A} receptor than 5-MeO-DMT [6,13], the increase of exposure to active metabolite could be additional risk when 5-MeO-DMT is co-abused with MAOI.

It should be noted that harmaline metabolism and pharmacokinetics is also affected by CYP2D6 status [18,35], which may increase the complexity of harmaline-5-MeO-DMT DDI. A faster elimination of harmaline leads to a lower exposure to harmaline in Tg-*CYP2D6* mice [18] that might counteract the effects of CYP2D6 on 5-MeO-DMT *O*-demethylation. Indeed, levels of bufotenine formed from 5-MeO-DMT were marginally different in wild-type and Tg-*CYP2D6* mice after co-administrated with harmaline (Table 5 and Fig. 4). Possible interpretations include a low dose (2 mg/kg, i.p.) of 5-MeO-DMT used in this study and the involvement of other murine P450s in 5-MeO-DMT *O*-demethylation [15]. Nevertheless, systemic exposure (AUC) to bufotenine metabolite was about 24% of that to 5-MeO-DMT in Tg-*CYP2D6* mice, whereas it was 15% in wild-type mice, indicating the influence of CYP2D6 status.

In summary, concurrent MAOI largely reduces 5-MeO-DMT depletion in human hepatocytes and 5-MeO-DMT systemic clearance in animal models. Meanwhile, MAOI shuns 5-MeO-DMT deamination metabolism to *O*-demethylation in vitro and in vivo, leading to an increased production and prolonged systemic exposure to active metabolite bufotenine, which is affected by CYP2D6 status. Together, our findings suggest that MAOI and CYP2D6 status may have significant impact on 5-MeO-DMT metabolism and pharmacokinetics, as well as the formation of bufotenine. The results would provide novel insights into biochemical determinants in 5-MeO-DMT pharmacokinetics and harmaline-5-MeO-DMT DDI, and advance our understanding of risks in 5-MeO-DMT intoxication.

Acknowledgements and disclosure

This project was supported by Award Number R01DA021172 from the National Institute On Drug Abuse, National Institutes of Health (NIH). The authors also thank the Pharmaceutical Sciences Instrumentation Facility at University at Buffalo for use of LC–MS

system that was obtained with Shared Instrumentation Grants S10RR014592 from the National Center for Research Resources, NIH.

References

[1] Ott J. Pharmanopo-psychonautics: human intranasal, sublingual, intrarectal, pulmonary and oral pharmacology of bufotenine. J Psychoactive Drugs 2001;33(3):273–81.
[2] McKenna DJ. Clinical investigations of the therapeutic potential of ayahuasca: rationale and regulatory challenges. Pharmacol Ther 2004;102(2):111–29.
[3] Yu AM. Indolealkylamines: biotransformations and potential drug–drug interactions. AAPS J 2008;10(2):242–53.
[4] Aghajanian GK, Marek GJ. Serotonin and hallucinogens. Neuropsychopharmacology 1999;21(2 Suppl.):16S–23S.
[5] Tricklebank MD, Forler C, Middlemiss DN, Fozard JR. Subtypes of the 5-HT receptor mediating the behavioural responses to 5-methoxy-N,N-dimethyltryptamine in the rat. Eur J Pharmacol 1985;117(1):15–24.
[6] Spencer Jr DG, Glaser T, Traber J. Serotonin receptor subtype mediation of the interoceptive discriminative stimuli induced by 5-methoxy-N,N-dimethyltryptamine. Psychopharmacology (Berl) 1987;93(2):158–66.
[7] Winter JC, Filipink RA, Timineri D, Helsley SE, Rabin RA. The paradox of 5-methoxy-N,N-dimethyltryptamine: an indoleamine hallucinogen that induces stimulus control via 5-HT1A receptors. Pharmacol Biochem Behav 2000;65(1):75–82.
[8] Krebs-Thomson K, Ruiz EM, Masten V, Buell M, Geyer MA. The roles of 5-HT1A and 5-HT2 receptors in the effects of 5-MeO-DMT on locomotor activity and prepulse inhibition in rats. Psychopharmacology (Berl) 2006;189(3):319–29.
[9] Brush DE, Bird SB, Boyer EW. Monoamine oxidase inhibitor poisoning resulting from Internet misinformation on illicit substances. J Toxicol Clin Toxicol 2004;42(2):191–5.
[10] Sklerov J, Levine B, Moore KA, King T, Fowler D. A fatal intoxication following the ingestion of 5-methoxy-N,N-dimethyltryptamine in an ayahuasca preparation. J Anal Toxicol 2005;29(8):838–41.
[11] DEA-2009-0008. Placement of 5-Methoxy-N,N-Dimethyltryptamine Into Schedule I of the Controlled Substances Act; 2009.
[12] Agurell S, Holmstedt B, Lindgren JE. Metabolism of 5-methoxy-N,-N dimethyltryptamine-14C in the rat. Biochem Pharmacol 1969;18(10):2771–81.
[13] Roth BL, Choudhary MS, Khan N, Uluer AZ. High-affinity agonist binding is not sufficient for agonist efficacy at 5-hydroxytryptamine2A receptors: evidence in favor of a modified ternary complex model. J Pharmacol Exp Ther 1997;280(2):576–83.
[14] McBride MC. Bufotenine: toward an understanding of possible psychoactive mechanisms. J Psychoactive Drugs 2000;32(3):321–31.
[15] Yu AM, Idle JR, Herraiz T, Kupfer A, Gonzalez FJ. Screening for endogenous substrates reveals that CYP2D6 is a 5-methoxyindolethylamine O-demethylase. Pharmacogenetics 2003;13(6):307–19.
[16] Zanger UM, Raimundo S, Eichelbaum M. Cytochrome P450 2D6: overview and update on pharmacology, genetics, biochemistry. Naunyn Schmiedebergs Arch Pharmacol 2004;369(1):23–37.
[17] Yu AM, Idle JR, Gonzalez FJ. Polymorphic cytochrome P450 2D6: humanized mouse model and endogenous substrates. Drug Metab Rev 2004;36(2):243–77.
[18] Wu C, Jiang XL, Shen HW, Yu AM. Effects of CYP2D6 status on harmaline metabolism, pharmacokinetics and pharmacodynamics, and a pharmacogenetics-based pharmacokinetic model. Biochem Pharmacol 2009;78(6):617–24.
[19] Yu A, Kneller BM, Rettie AE, Haining RL. Expression, purification, biochemical characterization, and comparative function of human cytochrome P450 2D6.1, 2D6.2, 2D6.10, and 2D6.17 allelic isoforms. J Pharmacol Exp Ther 2002;303(3):1291–300.
[20] Zhang WY, Tu YB, Haining RL, Yu AM. Expression and functional analysis of CYP2D6.24, CYP2D6.26, CYP2D6. 27, and CYP2D7 isozymes. Drug Metab Dispos 2009;37(1):1–4.
[21] Jiang XL, Shen HW, Yu AM. Pinoline may be used as a probe for CYP2D6 activity. Drug Metab Dispos 2009;37(3):443–6.
[22] Corchero J, Granvil CP, Akiyama TE, Hayhurst GP, Pimprale S, Feigenbaum L, et al. The CYP2D6 humanized mouse: effect of the human CYP2D6 transgene and HNF4alpha on the disposition of debrisoquine in the mouse. Mol Pharmacol 2001;60(6):1260–7.
[23] Shen HW, Jiang XL, Yu AM. Development of a LC–MS/MS method to analyze 5-methoxy-N,N-dimethyltryptamine and bufotenine: application to pharmacokinetic study. Bioanalysis 2009;1(1):87–95.
[24] Yu AM, Granvil CP, Haining RL, Krausz KW, Corchero J, Kupfer A, et al. The relative contribution of monoamine oxidase and cytochrome p450 isozymes to the metabolic deamination of the trace amine tryptamine. J Pharmacol Exp Ther 2003;304(2):539–46.
[25] de la Torre R, Farre M, Mathuna BO, Roset PN, Pizarro N, Segura M, et al. MDMA (ecstasy) pharmacokinetics in a CYP2D6 poor metaboliser and in nine CYP2D6 extensive metabolisers. Eur J Clin Pharmacol 2005;61(7):551–4.
[26] Kim H, Sablin SO, Ramsay RR. Inhibition of monoamine oxidase A by beta-carboline derivatives. Arch Biochem Biophys 1997;337(1):137–42.
[27] Ott J. Pharmepena-psychonautics: human intranasal, sublingual and oral pharmacology of 5-methoxy-N,N-dimethyl-tryptamine. J Psychoactive Drugs 2001;33(4):403–7.
[28] Halberstadt AL, Buell MR, Masten VL, Risbrough VB, Geyer MA. Modification of the effects of 5-methoxy-N,N-dimethyltryptamine on exploratory behavior in rats by monoamine oxidase inhibitors. Psychopharmacology (Berl) 2008;201(1):55–66.
[29] Kamata T, Katagi M, Kamata HT, Miki A, Shima N, Zaitsu K, et al. Metabolism of the psychotomimetic tryptamine derivative 5-methoxy-N,N-diisopropyltryptamine in humans: identification and quantification of its urinary metabolites. Drug Metab Dispos 2006;34(2):281–7.
[30] Narimatsu S, Yonemoto R, Saito K, Takaya K, Kumamoto T, Ishikawa T, et al. Oxidative metabolism of 5-methoxy-N,N-diisopropyltryptamine (Foxy) by human liver microsomes and recombinant cytochrome P450 enzymes. Biochem Pharmacol 2006;71(9):1377–85.
[31] Narimatsu S, Yonemoto R, Masuda K, Katsu T, Asanuma M, Kamata T, et al. Oxidation of 5-methoxy-N,N-diisopropyltryptamine in rat liver microsomes and recombinant cytochrome P450 enzymes. Biochem Pharmacol 2008;75(3):752–60.
[32] Sitaram BR, McLeod WR. Observations on the metabolism of the psychotomimetic indolealkylamines: implications for future clinical studies. Biol Psychiatry 1990;28(10):841–8.
[33] Sitaram BR, Lockett L, Talomsin R, Blackman GL, McLeod WR. In vivo metabolism of 5-methoxy-N,N-dimethyltryptamine and N,N-dimethyltryptamine in the rat. Biochem Pharmacol 1987;36(9):1509–12.
[34] Fuller RW, Snoddy HD, Perry KW. Tissue distribution, metabolism and effects of bufotenine administered to rats. Neuropharmacology 1995;34(7):799–804.
[35] Yu AM, Idle JR, Krausz KW, Kupfer A, Gonzalez FJ. Contribution of individual cytochrome P450 isozymes to the O-demethylation of the psychotropic beta-carboline alkaloids harmaline and harmine. J Pharmacol Exp Ther 2003;305(1):315–22.